ELSEVIER

Journal of Orthopaedic Research 20 (2002) 222–232

Journal of Orthopaedic Research

www.elsevier.com/locate/orthres

Plantar impact causing midfoot fractures result in higher forces in Chopart's joint than in the ankle joint

M. Richter [a,*], B. Wippermann [a], H. Thermann [d], G. Schroeder [c], D. Otte [b], H.D. Troeger [c], C. Krettek [a]

[a] *Trauma Department, Hannover Medical School, Hannover, Germany*
[b] *Accident Research Unit, Hannover Medical School, Hannover, Germany*
[c] *Department of Forensic Medicine, Hannover Medical School, Hannover, Germany*
[d] *ATOS Center for Knee and Foot Surgery, Heidelberg, Germany*

Received 5 June 2001; accepted 22 June 2001

Abstract

Purpose. Force effect (impact, extent of foot compartment deformation) and result (fracture pattern) for midfoot fractures in car occupants is known. An analysis of the processes *in* the foot was intended to improve car safety.

Materials and methods. Eleven fresh, unfrozen, unpreserved intact human cadavers (age: 36.8 (16–61) years, gender: male, race: Caucasian) were studied 24–72 h after death. In 3 cadavers (5 feet) the experimental design was established: entire cadaver fixed on a special tray in supine position, pendulum with bar impactor hitting the foot plantar to Lisfranc's joint. A custom-made pressure sensor was inserted in the ankle (A), talonavicular (TN) and calcaneocuboid (CC) joints (resolution: 1 cm^2, sampling rate: 500/s).

Results. Sixteen feet were measured; midfoot fractures were induced in 11 feet. The maximum pressure amounted to 1.22–2.55 MPa (2.04 ± 0.412) at 0.005–0.195 s (0.067 ± 0.059) after impact. The maximum pressure occurred in 8 (50%) cases in the ankle, in 7 (44%) of the TN and 1 (6%) of the CC joints. A comparison of the first 200 pressure samples after impact of all sensor fields resulted in higher forces in Chopart's joint than in the ankle (*t*-test: $p < 0.001$). These force differences were higher in cases *with* midfoot fractures (mixed model analysis of variance: $p = 0.003$).

Conclusion. Due to considerable forces in Chopart's joint we recommend a modification of the actual crash test dummy lower extremity model with an additional load cell that detects forces in the longitudinal direction of the foot axis.

Keywords: Midfoot fracture; Plantar impact; Joint pressure; Ankle; Chopart

Introduction

Among the injuries in the foot region, midfoot fractures are still problematic in both diagnosis and treatment and result in a high degree of long-term morbidity [1,2,9,14,16,24,29]. Midfoot fractures are uncommon and predominantly occur in motor vehicle collisions [3,29]. Despite significant improvements in automobile safety, the incidence and severity of fractures of the foot region in car occupants has remained the same and especially midfoot fractures step in the foreground [4,5,7,8,13,20,21]. Further improvements under special consideration of the foot compartment are necessary. Force effect (impact, extent of foot compartment deformation) and result (fracture pattern, soft tissue damage) for midfoot fractures in car occupants are known [13,20,21]. However the exact injury mechanism is unclear. Previous experimental settings with high-speed cameras, accelerometers and/or load cells only detected movements of the surface and indirect forces effecting the foot [5]. Based on these investigations, actual crash test models have been developed [11,17]. It is questionable whether this design is appropriate to detect all fractures in the foot region. In particular, the lack of sensing in the midfoot area may result in an insufficient detection of midfoot fractures. To further evaluate this question, a detailed analysis of the injury mechanism of midfoot fractures is obligatory.

* Corresponding author. Present address: Unfallchirurgische Klinik, Medizinische Hochschule Hannover, Carl-Neuberg-Strasse 1, 30625 Hannover, Germany. Tel.: +49-511-532-2050; fax: +49-511-532-5877.
E-mail address: richter.martinus@mh-hannover.de (M. Richter).
URL: http://www.martinusrichter.de

0736-0266/02/$ - see front matter
PII: S0736-0266(01)00096-1

We intended to analyze the processes *in* the foot at the time of the injury and to determine the injury mechanism more precisely. A unique method with permanent registration of bone motion and joint pressure distribution in the foot should be used and established.

Materials and methods

Eleven fresh, unfrozen, unpreserved intact human cadavers (age: 36.8 (16–61) years, gender: male, race: Caucasian) were studied 24–72 h after death. The cadavers were stored in standard refrigerators in the Institute for Forensic Medicine. An autopsy had been performed in all cases 1–24 h before testing. Prior to testing, each cadaver was warmed to room temperature, examined and radiographs performed to determine the evidence of abnormalities, deformities and injuries. Exclusion criteria were not detected in the cadavers of the study group. The rigor mortis was not interrupted (see Fig. 1).

The method for inducing midfoot fractures was developed and optimized in a preliminary testing of three cadavers (five trials in five feet, the first specimen was unilaterally tested) (Table 1). Midfoot fractures could be reproducibly induced using the following criteria.

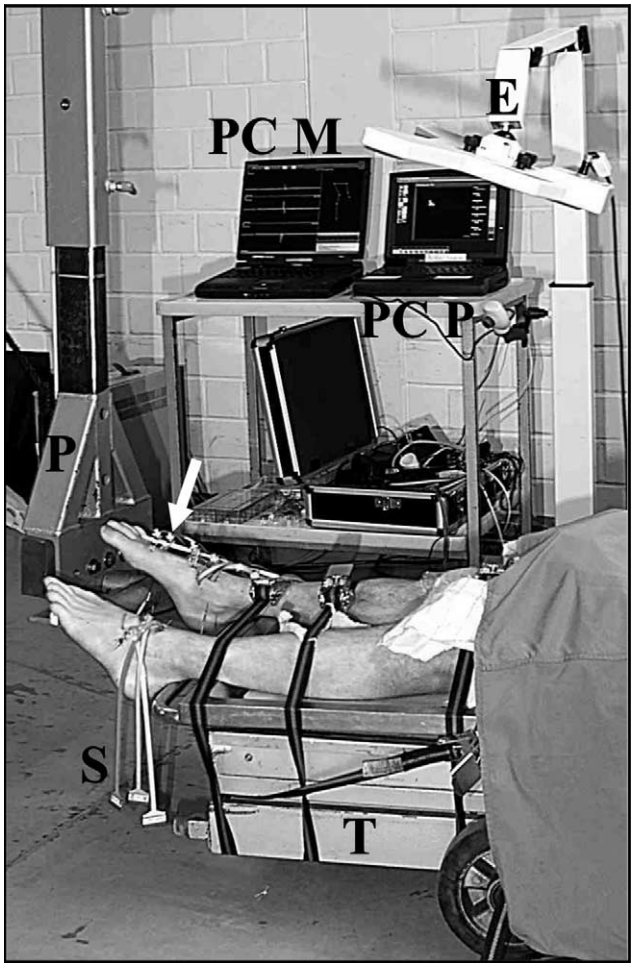

Fig. 1. Setting; P, pendulum; E, ultrasound emitter; PC P, personal computer for control of pressure measurement; PC M, personal computer for motion tracking system; white arrow, ultrasound microphones (with adaptors attached to K-wires); S, pressure sensor cables (sensors in joints); T, tray for cadaver adjustment and fixation.

Only one foot was tested at a time. The cadaver was positioned in the supine position on a tray with adjustable height (model custom-made; Workshop Hannover Medical School, Hannover, Germany, length: 200 cm, width: 80 cm, height: 30–180 cm, weight: 100 kg). The cadavers were fixed to the tray with three straps, and the tray was fixed to columns of the laboratory with two straps. The distance between floor and distal tip of the fibula was adjusted to 35 cm, with the tip at the edge of the tray. A custom-made, length adjustable pendulum was fixed at the ceiling 2.8 m above the floor. The impactor bar of the pendulum had a diameter of 7.0 cm. The effective weight of the impactor bar amounted to 50 kg. The sole of the foot touched the impactor bar slightly when the pendulum was in a dependent position. The plane of the pendulum was in the midaxial line of the foot. The length of the pendulum was adjusted so that foot strike was plantar at Lisfranc's joint. The leg was fixed with straps in neutral position of lower leg rotation, i.e. the longitudinal axis of the foot was parallel to the sagittal plane, and the foot was in slight inversion and in approx. 20° ankle plantar-flexion (Table 1). The foot position was maintained in this position by textile straps as necessary. The pendulum was lifted to an effective height of 2.3 m (i.e., height difference of 2.3 m) and then was allowed to swing freely, striking the foot. The energy of the pendulum totaled to 1130 J at impact.

Pressure distribution measurement system

Custom-made pressure sensors (Novel, Munich, Germany) were inserted in the ankle and Chopart's joint (one sensor each in the talonavicular and calcaneocuboid joints). The size of the sensors measured 3×3 cm^2 for the ankle, and 2×2 cm^2 for the talonavicular and calcaneocuboid joints. The sensors contained a rectangular array of 10 mm $\times$ 10 mm transducers. The thickness of the sensor measured 1 mm. The sensors were sealed in a clear, fluid resistant plastic tape (model Scotch Brand Tape; 3M, St. Paul, MN, USA) to guard against humidity. The manufacturer calibrated the sensors such that the load-signal relationship of each transducer was determined individually. The pressure range was 0–3 MPa. The accuracy of each sensor was rated as better than 5% and hysteresis was less than 3% providing an unvarying measurement even in high sampling rates [6,10,15,18]. The sensors were connected to a standard receiver (model pliance mobile™; Novel, Munich, Germany) which was in turn connected with the RS 232 serial interface of an IBM compatible laptop computer. Standard software (model Pliance-m expert™ V6.3-4/2000; Novel, Munich, Germany) was utilized. The sampling rate was 500 per second. For analysis the pressure data were converted to a digital image where the pixel color temperature was linearly related to pressure magnitude, and the pressure values were given numerical equivalence. Equipment testing and calibration was performed between each second test (between each cadaver). The sensors were inserted into the cadaver feet through three incisions. The ankle joint was exposed through an anterior approach; the talonavicular joint was exposed through a dorsomedial approach, and the calcaneocuboid joint through a dorsolateral approach (Fig. 2). The ligaments were retained, the joint capsules were minimally violated, and the incision repaired with deep suture (model Mersilene™ No. 0; Ethicon, Norderstedt, Germany).

Based on pressure values a calculation of joint forces was performed. Pressures in 1 cm^2 areas were measured and the corresponding force effecting this area was calculated (For example a pressure of 2 MPa corresponds to a force of 200 N affecting the 1 cm^2 area (2 MPa = 2,000,000 Pa = 2,000,000 N/m^2 = 200 N/cm^2)). The force affecting the entire sensor or joint was considered to be the sum of forces affecting the single areas at the same time.

Motion tracking system

The spatial orientation of bones was recorded with an ultrasound measurement system (model CMS HS™; Zebris, Tuebingen, Germany). Standard 2 mm K-wires were drilled into the corresponding bones (tibia, talus, calcaneus, navicular, cuboid, metatarsal 1, and metatarsal 5) under image intensifier control (model Fluoroscan III Imaging System™; Karus, Wennigsen, Germany). The microphones were included in the measurement system (model standard microphone; Novel, Munich, Germany, cylindrical shape, height 10 mm, diameter: 5 mm, weight: 1 g). Two different settings were performed:

Table 1
Testing protocol[a]

No.	Cadaver no.	Age	Height (cm)	Weight (kg)	Cause of death	Side	Foot morphology	Flexion	Supination	Rigor mortis	Degree of arthritis	Ultrasound microphone	Pressure sensors	Fracture foot/midfoot	Instability	Other injury
P1	1	36	190	86	MVA	r	Normal	30	20	Distinct	None	0	0	n	n	n
P2	2	41	169	96	Bleeding upper gastrointestine	r	Normal	30	15	Distinct	Slight	0	0	Fx Base MT 5, Fx post. talar processus	n	n
P3						l	Normal	35	10	Distinct	Slight	0	0	Trans-navicular-calcanear Chopart fracture dislocation, Fx Base MT 5, Fx post. talar processus	Chopart, Lisfranc	n
P4	3	27	175	85	Suicidal fall	r	Normal	30	10	Distinct	None	0	0	n	n	n
P5						l	Normal	30	20	Distinct	None	0	0	Fx post. talar processus, Medial avulsion naviculare	n	n
1	4	28	169	88	MVA	r	Cavus	30	10	Distinct	None	7	3	Lisfranc fracture dislocation (with Fx naviculare, MT 5)	Lisfranc	n
2						l	Cavus	30	10	Distinct	None	7	3	Fx talar neck, trans-navicular Chopart fracture dislocation	ankle-calcanear, Chopart	n
3	5	53	163	86	Cardiac infarction	r	Normal	20	10	Moderate	None	7	3	Fx navicular, Fx post. talar processus	Chopart	n
4						l	Normal	20	10	Moderate	None	7	3	Jones Fx, Fx naviculare, Fx post. talar processus	n	n
5	6	28	183	99	MVA	r	Varus	20	20	Moderate	None	7	3	n	n	n
6						l	Varus	20	20	Moderate	None	7	3	n	n	n
7	7	28	178	93	MVA	r	Normal	20	10	Moderate	None	7	3	n	ankle-calcanear, Chopart	n
8						l	Normal	20	10	Moderate	None	7	3	n	ankle-calcanear, Chopart	n
9	8	61	165	52	Suffocation	r	Normal	20	0	Moderate	Moderate	7	3	Trans-calcanear Chopart fracture dislocation, avulsion Fx MT 5	ankle-calcanear, Chopart	Fx tibia
10						l	Normal	20	0	Moderate	Moderate	10	3	Trans-calcanear-talar Chopart fracture dislocation, Tongue type calcaneus Fx	ankle-calcanear, Chopart	Fx medial malleolus

11	9	35	177	72	MVA	r	Planus	20	10	Distinct	None	7	3	Lisfranc fracture dislocation with Fx Cuboid, avulsion Fx MT 5	ankle-calcanear, Lisfranc	n
12						l	Planus	20	10	Distinct	None	10	3	n	ankle-calcanear, Chopart	n
13	10	16	177	82	Industrial accident	r	Normal	10	0	Mild	None	7	3	Fx naviculare, avulsion calcaneus	ankle-calcanear	n
14						l	Normal	10	0	Mild	None	10	3	Trans-calcanear Chopart fracture dislocation	ankle-calcanear, Chopart	n
15	11	45	180	100	Cardiac infarction	r	Normal	0	0	Mild	None	0	3	Trans-navicular Chopart fracture dislocation, avulsion calcaneus	ankle-calcanear, Chopart	Fx medial malleolus
16						l	Normal	0	0	Mild	None	0	3	Trans-navicular Chopart fracture dislocation, avulsion calcaneus	ankle-calcanear, Chopart	Fx medial malleolus

[a] Case nos. of preliminary study are specified with a "P"; Fx, fracture; MVA, motor vehicle accident.

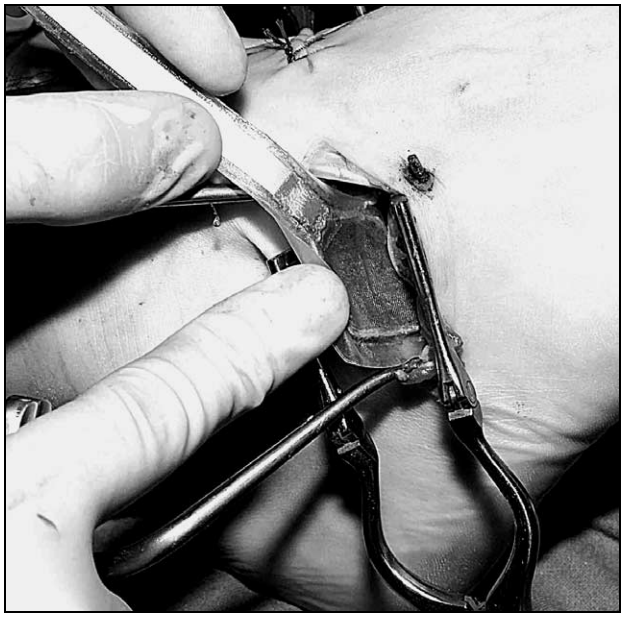

Fig. 2. Insertion of a pressure sensor (2×2 cm^2) in the calcaneocuboid joint (CC) (forefoot at right upper corner, heel at lower middle).

1. All seven bones were equipped with one single microphone (uniaxial) with an adapter (model custom-made, material Plexiglas™ (Rohm and Haas, Pennsylvania, PA, USA); Workshop Hannover Medical School, Hannover, Germany, rectangular shape, height: 20 mm, width: 10 mm, length: 10 mm, weight: 3 g, possibility of microphone fixation in four different spatial orientations; Fig. 3, right side).
2. The tibia was equipped with one single microphone. K-wires placed in the talus, naviculare and cuboid were each connected to three microphones (triaxial) via a star-shaped adapter (model custom-made, material Plexiglas™; Workshop Hannover Medical School, Hannover, Germany, microphones were situated at the edges of an equilateral triangle with a side length of 50 mm, a fixation point for the K-wire in the center, maximum height of adapter 10 mm, and weight 12 g; Fig. 3, center).

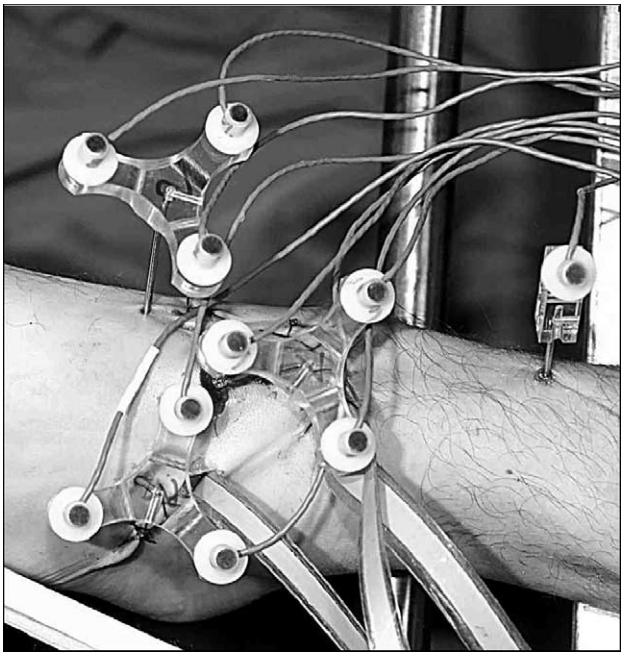

Fig. 3. Microphones of the motion tracking system, adapters, and K-wires.

The rectangular distance between bone center and single microphones was 2 cm, and between the triple microphones and bone center 5 cm. These distances were measured before and after the tests (remark: no statistical differences were observed in the positions before and after the tests). The microphones were connected to the central unit of the measurement system with thin electrical cables. The ultrasound impulses were emitted by a transducer (model MH HS 3™; Zebris, Tuebingen, Germany) which was also connected to the central unit. The distance between the transducers and the microphones was approximately 1 m. The absolute spatial accuracy of the system was rated as 0.1 mm, resolution as 50 μm and the angular accuracy for the triaxial sensors as less than 1° in all six degrees of freedom. This was reported by the manufacturer and independently by Wulker et al. [28]. The data were transmitted from the central unit to an IBM compatible laptop. The control software (model Win Data™ V2.19.20; Zebris, Tuebingen, Germany) was installed on the computer. The sampling rate of the system was 100 per second. A software analysis indicated three different course curves in three different windows for each microphone/bone unit in the *x*-, *y*- or *z*-plane. A virtual model in three-dimensional view was also displayed. All data were exported and stored in ASCII files for further statistical analysis. Due to data loss in all testing procedures from 0.02 to 0.08 s after impact only the complete displacement of the bones due to the impact was analyzed and not the motion during the impact. For this purpose, changes in the spatial positions (for uniaxial and triaxial sensors) and/or angles (for triaxial sensors) of the microphone/bone units between positions *before* (at 0 s) and *after* the impact and the bone motion due to the impact (at 0.3 s) were evaluated. In the last two tests (no. 15 and 16) the motion tracking system failed.

Testing sequence

The K-wires and pressure sensors were inserted into both feet. The adapters and the microphones were connected to the K-wires. The cadaver was aligned to the pendulum and secured. The sensors and microphones were connected to the central units. The pendulum was lifted to the starting point. The central units of the pressure and motion tracking systems were synchronized by a TTL signal via a thin electrical cable. The pendulum was allowed to swing freely and impact the foot. The procedure was repeated for the opposite extremity. The feet were clinically examined and all signs of injury including instabilities were recorded. Both feet had radiographs obtained for later evaluation of fractures.

Statistical analysis and hypothesis testing

Statistical analysis included paired *t*- or Wilcoxon-test for differences of maximum pressure or force. The forces over time were analyzed with a mixed model analysis of variance with the random effect "cadaver" and the fixed effect "incidence of midfoot fracture". The null hypothesis at the $p < 0.05$ level was that there is no difference between the pressure and force in the ankle versus Chopart's joint.

Results

Injuries

Table 1 indicates the testing protocol. The mean height of the cadavers was 174 (163–190) cm and the mean weight 84 (52–100) kg. Fractures in the midfoot region occurred in 11 (69%) of 16 feet. Fracture dislo-

Table 2
Comparison between cadavers with bilateral midfoot fractures and cadavers without or with unilateral midfoot fractures

	Cadavers with *bilateral* midfoot fractures (Nos. 4, 5, 8, 10, 11)	Cadavers with *unilateral* of *without* midfoot fractures (Nos. 6, 7, 9)	*t*-test
Age	40.6 ± 18.4 years	30.3 ± 4.0 years	$p = 0.288$
Height	170.8 ± 7.4 cm	179.3 ± 3.2 cm	$p = 0.138$
Weight	81.6 ± 17.9 kg	88.0 ± 14.2 kg	$p = 0.599$

cations were diagnosed in 8 cases (Chopart: $n = 6$, Lisfranc: $n = 2$). Age, height and weight did not differ significantly between cadavers with ($n = 5$) and without ($n = 3$) bilateral midfoot fractures (Table 2).

Joint pressure and forces

The pressure measurements of the ankle, talonavicular (TN) and calcaneocuboid (CC) joints are indicated in Table 3. The maximum pressure that was registered at one of the total 17 sensor fields (ankle: 3×3, TN: 2×2, CC: 2×2) amounted to 1.22–2.55 MPa (2.04 ± 0.412). The time after impact of the maximum pressure was 0.005–0.195 s (0.067 ± 0.059). The maximum pressure of one complete testing procedure was measured in 8 (50%) of cases at the ankle, in 7 (44%) at the TN and in 1 (6%) at the CC joint. The maximum pressure at the ankle ($n = 8$) was measured in the ventral third of the joint in two cases, at the central third in three cases and at the dorsal third in four cases. The maximum pressure in Chopart's joint ($n = 8$) was situated in three cases at the dorsal half and in five cases at the plantar half. The maximum force (maximum pressures sum of all sensor fields at the same time) ranged from 381 to 1458 N (947.9 ± 266.7). The maximum force in Chopart's joint was higher than the maximum force in the ankle in 10 (62.5%) of cases, and the mean difference amounted to 115.1 N (± 425.1 N). The differences between the maximum forces in ankle and Chopart's joints were not significant (*t*-test: $p = 0.519$). No differences in the maximum forces occurred when comparing the feet with ($n = 11$) or without ($n = 5$) midfoot fractures (Wilcoxon test: $p = 0.352$). The comparison of the first 200 pressure samples after impact (i.e., 0 to 0.4 s, data not shown) of all 17 sensor fields (ankle, $n = 9$; Chopart, $n = 8$) resulted in significantly higher forces in Chopart's joint (sum of all 8 sensors) than in the ankle (sum of all 9 sensors) (*t*-test: $p < 0.001$). These force differences were significantly higher in cases with midfoot fractures ($n = 11$) in comparison to cases without midfoot fractures ($n = 5$) (mixed model analysis of variance of the first 200 pressure samples after impact with random effect "cadaver" and fixed effect "incidence of midfoot fracture" of forces in ankle (sum of all 9 sensors) and Chopart's joint (sum of all 8 sensors) $p = 0.003$).

The null hypothesis was rejected.

Bone motion

The measurement values were missing in all cases from 0.02 to 0.08 s after impact. Table 4 indicates the differences of the spatial bone position between 0 and 0.3 s after impact. Seven bones (as described under 1 in the methods) were measured in 11 cases, and four bones (as 2) in three cases. A motion perpendicular up or down, towards lateral, medial, proximal or distal was registered in all bones with one microphone. The mean values of all cases (bones with one microphone) match to a motion towards lateral and proximal in all 7 bones, up in 6 bones and down in 1 (navicular). The rotation in six degrees of freedom, i.e. abduction/adduction, inversion/eversion and plantar-flexion/dorsal-extension, was registered in the bones with three microphones. The mean values of all these cases (bones with three microphones) match to an abduction and dorsal-extension in all three bones, eversion in two and inversion in one (talus).

Discussion

Biomechanical crash test model for midfoot fractures and fracture dislocations

We introduce a biomechanical model for simulation of midfoot fractures and an exact analysis of the injury mechanism. A reproducible induction of midfoot fractures in intact human cadavers can be achieved with this model. An experimental setting to induce midfoot fractures is not reported in the literature except for Lisfranc's joint fracture dislocations in studies from Wiley and Wilson in the early 1970s [26,27]. Wiley clinically analyzed the injury mechanism of eleven Lisfranc's joint injuries [26]. He described the injury mechanism as an 'acute plantar-flexion injury'and tried to reproduce this mechanism experimentally on cadaver specimens. A simple press machine was designed to apply force along the axis of the tibia with the ankle fixed in a position of maximum plantar-flexion. Wiley was in fact the first who reported an experimental induction of Lisfranc's joint injuries. However, the injury mechanism was not further analyzed by force or motion measurements. Wilson performed an experimental study

Table 3
Maximum pressures (MPa) and forces (N) in the ankle, talonavicular (TN) and calcaneocuboid (CC) joint, and time when occurring after the impact (s)

No.	Maximum pressure (MPa)	Time maximum pressure (s)	Field maximum pressure (MPa)	Sensor maximum pressure	Maximum force (N)	Time maximum force (s)	Ankle maximum force (N)	Ankle maximum time (s)	TN maximum force (N)	TN maximum time (s)	CC maximum force (N)	CC maximum time (s)	Maximum force TN + CC–Ankle (N)
1	1.22	0.105	b3	TN	381	0.003	71	0.010	235	0.350	139	0.060	303
2	2.04	0.144	a1,a2	Ankle	646	0.007	551	0.016	72	0.036	216	0.036	−263
3	2.10	0.005	a9	Ankle	1073	0.042	861	0.045	180	0.005	112	0.025	−569
4	1.83	0.013	a4	Ankle	815	0.013	604	0.013	165	0.035	108	0.010	−331
5	2.15	0.063	c4	CC	621	0.063	248	0.006	306	0.019	296	0.003	354
6	1.33	0.008	a3,a5	Ankle	796	0.008	577	0.008	183	0.024	183	0.018	−211
7	1.88	0.109	a7	Ankle	1060	0.033	722	0.093	237	0.023	360	0.033	−125
8	2.07	0.006	a9	Ankle	1108	0.023	556	0.023	321	0.017	303	0.023	68
9	2.55	0.016	b4	TN	1157	0.016	691	0.082	340	0.119	612	0.016	261
10	2.33	0.005	b2	TN	1458	0.031	796	0.003	548	0.009	496	0.131	248
11	1.60	0.095	b3	TN	1108	0.012	536	0.090	248	0.020	604	0.020	316
12	2.55	0.195	b2	TN	892	0.023	296	0.023	442	0.195	76	0.032	222
13	1.83	0.116	b3	TN	987	0.116	108	0.110	549	0.116	508	0.098	949
14	2.55	0.017	a6	Ankle	1277	0.017	1020	0.017	360	0.033	188	0.038	−472
15	2.47	0.072	a9	Ankle	939	0.025	418	0.072	311	0.021	384	0.114	277
16	2.08	0.100	b1	TN	848	0.149	228	0.149	322	0.100	720	0.173	814
M	2.04	0.067			947.9	0.043	517.7	0.054	301.2	0.070	331.6	0.052	115.1
SD	0.41	0.059			266.7	0.061	272.8	0.064	131.4	0.092	204.0	0.050	425.4

Maximum force: maximum pressure sum of all 17 sensor fields at the same time. Sensor fields: ankle, a1–a9, a1–a3: ventral third, a4–a6: central third, a7–a9: dorsal third, a1/a4/a7: left third, a2/a5/a8: middle third, a3/a6/a9: right third; TN: b1–b4, CC: c1–c4, b1, 2/c1, 2: dorsal half, b3, 4/c3, 4: plantar half, b1, 3/c1, 3: left half, b2, 4/c2, 4: right half. M: mean values, S.D.: standard deviation.

Table 4
Differences of bone positions between time 0 and 0.3 s after impact

Bone	Dimension (SI unit)	*n*	Mean	S.D.
Tibia	*X* (mm)	14	4.2	24.2
	Y (mm)	14	29.6	97.7
	Z (mm)	14	20.2	64.23
Talus	*X* (mm)	11	2.2	28.1
	Y (mm)	11	24.5	104.0
	Z (mm)	11	25.5	75.2
	Abduction/adduction (°)	3	10.2	34.7
	Inversion/eversion (°)	3	5.8	13.2
	Plantar-flexion/dorsal-extension (°)	3	−11.5	33.8
Calcaneus	*X* (mm)	11	7.7	39.7
	Y (mm)	11	27.7	96.3
	Z (mm)	11	21.8	55.0
Navicular	*X* (mm)	11	−5.4	24.2
	Y (mm)	11	29.7	97.7
	Z (mm)	11	25.0	64.23
	Abduction/adduction (°)	3	42.5	60.7
	Inversion/eversion (°)	3	−16.3	19.5
	Plantar-flexion/dorsal-extension (°)	3	−48.1	38.4
Cuboid	*X* (mm)	11	10.6	37.8
	Y (mm)	11	27.4	98.7
	Z (mm)	11	39.6	63.6
	Abduction/adduction (°)	3	5.4	28.7
	Inversion/eversion (°)	3	−6.9	13.8
	Plantar-flexion/dorsal-extension (°)	3	−17.9	24.3
Metatarsal 1	*X* (mm)	11	1.5	34.6
	Y (mm)	11	26.2	115.0
	Z (mm)	11	25.5	73.4
Metatarsal 5	*X* (mm)	11	13.4	60.1
	Y (mm)	11	40.0	111.0
	Z (mm)	11	41.0	75.4

Dimensions: *X*, positive value: motion up, negative: down; *Y*, positive: towards lateral, negative: towards medial; *Z*, positive: towards proximal, negative: towards distal; Rotation: positive: abduction, inversion, plantar-flexion, negative: adduction, eversion, dorsal-extension.

on eleven preserved feet based on his clinical analysis of Lisfranc's joint injury [27]. Manual strains were applied to the forefoot while the hindfoot was held rigid. Manual force was used only in crushing experiments. He also did not use any form of force of motion measurement. Although Wilson and Wiley stated that in car accidents people in front seats have their feet fixed in plantar-flexion on the sloping ground and are vulnerable to Lisfranc's joint injuries, we found a different predominant injury mechanism in our accident analyses [19]. In our technical and clinical analysis of 261 car front seat occupants with fractures of the foot region, the typical accident mechanism for midfoot fractures including Lisfranc's joint injuries was a plantar force in *slight* plantar-flexion. Therefore, we tried to simulate this injury mechanism in our experimental study. Although a pendulum and not a real car crash was used, similar fracture patterns as observed in real-world car crashes could be induced [21]. The position of the foot in the setting (neutral lower leg rotation, neutral in-/eversion and approximately 20° ankle plantar-flexion) was adjusted to a position which was found to be a typical situation for car drivers at the beginning of a crash [19]. The rigor mortis was not broken and this situation was postulated to simulate muscle pretension.

Conventional motion and force registration

The actual gold-standard for the analysis of the injury mechanism in cadaver testing is high-speed video cameras and load cells/accelerometers that were attached to the surface of the cadaver [5]. The motion of the skin, indirect forces and acceleration outside the foot can be registered with these methods. However, the detection of direct forces and motion of bones is required to analyze the injury mechanism in detail. In a modified setting by Crandall et al., a load cell was introduced in an artificial gap of the tibia shaft (Auto Safety Laboratory,

University of Virginia, Charlottesville, Virginia, USA). But even with this procedure, the forces that occurred in the foot could not be directly detected.

With the introduced setting, direct forces in the foot, i.e., joint pressure/forces and bone motion should be registered:

Bone motion registration

An ultrasound-based motion tracking system (Zebris, Tuebingen, Germany) was utilized for the registration of bone motion in our study. The system has been successfully used for gait assessment and in bone motion registration in a cadaver shoulder model [28]. However, missing values occurred in all testing procedures between 0.02 and 0.08 s after impact. An indepth analysis of this finding showed that the pendulum emitted ultrasound at impact, which was considered to disturb the system. Therefore, the motion analysis of bones with the introduced system following an impact by a pendulum cannot be recommended. The analysis also showed that the system measures either nothing or accurate. Therefore, the missing values between 0.02 and 0.08 s have no influence on the accuracy of earlier or later registrations. The system allows a highly accurate determination of three-dimensional spatial position of bones before and after impact and the motions caused by the impact, i.e. the total displacement caused by the impact. The mean total displacements of the bones in all tests between the times 0 and 0.3 s were as follows: all bones had moved proximally and laterally and had rotated comparable to an abduction and dorsal-extension. All but one bone had moved up and rotated similar to eversion. The navicular had moved down and the talus had rotated similar to inversion. The reading was performed at 0.3 s, because at this time the motions due to the impacts were finished in all cases. At 0.1 or 0.2 s some of the specimens did still move. Due to the lack of registration at the most interesting times shortly after impact, a further analysis of the results was not performed. Based on our experience with the introduced motion tracking system, we do not recommend its use for high-speed crash analysis.

Joint pressure and force registration

To date, pressure sensitive films are the standard for joint pressure measurement (Fujifilm Prescale™, Mitsui, NY, USA) [23,25]. This method is useful for the assessment of static pressure forces, because the films only detect the maximum pressure over the entire measurement procedure. Sensors with repeated registration are necessary to assess dynamic pressure and forces. A sampling rate of 1000/s would be desirable, as it is typical for crash testing [12]. The sensors we used had a sampling rate of 500/s, which is concise for high-speed impacts, but much more appropriate than standard static pressure films. The resolution and sensors we used were much lower (1 cm^2) than pressure sensitive films provide (1 mm^2). However, the rectangular array of the sensor fields (2×2 or 3×3) allows an assessment of force and pressure distribution. The sensors that we used cannot measure shearing forces as well as the common pressure films. The objectivity and reliability of the sensors is comparable to the Fuji™ films. The validity of the measured joint pressure and forces is questionable for our system and cannot be determined because of the lack of a valid method for permanent pressure measurement to compare with. The literature does not provide any corresponding data as far as we know. The objectivity and reliability of our system allows a sufficient comparison of pressure and forces between measured joints, even if the validity may not be given. Consequently, our null hypothesis was formulated that there is no force or pressure difference between the ankle and Chopart's joint. A rejection of the null hypothesis was expected with higher forces and pressures in the ankle joint, because the direction of the pendulum's impact was approx. perpendicular to the ankle joint and parallel to Chopart's joint surfaces. Surprisingly, in 62.5% ($n = 10$) of the cases the maximum forces were higher in Chopart's joint than in the ankle, but the differences of the maximum forces between ankle and Chopart's joint were not significant. The forces in Chopart's joint were significantly *higher* than the forces in the ankle when comparing the first 200 pressure samples (0–0.4 s) after impact. The maximum forces/pressures did not differ significantly between feet with and without midfoot fractures. A trend for higher age and lower height and/or weight in those cadavers with bilateral midfoot fractures ($n = 5$) in comparison to those without or with unilateral midfoot fractures ($n = 3$) was observed. Despite the fact these differences were not significant, the "cadaver" was considered to be a considerable factor for the "incidence of midfoot fracture". To eliminate the influence of the cadaver, a mixed model analysis of variance of the first 200 pressure samples after impact with random effect cadaver and fixed effect "incidence of midfoot fracture" was performed to isolate the force differences between ankle (sum of all nine sensors) and Chopart's joint (sum of all 8 sensors). This analysis showed significantly higher force differences between Chopart's joint and ankle for cases with midfoot fractures in comparison to cases without midfoot fractures. The null hypothesis was rejected, not due, however, to higher forces in the ankle as expected, but rather, due to higher forces in Chopart's joint. The significant differences could be detected with a comparison of measurements over time and not with a comparison of maximum values only. The large difference in the time to maximum pressure is not a remarkable finding in our view. When analyzing the whole data

set (data not shown), the maximum pressure alone is not a main factor, because the pressure had several peaks early and late afterimpact. Besides, the maximum pressure was in most cases not considerably higher than pressures at other times. The large difference in the time to max pressure moreover represents the high variance in the pressure distribution in this type of injury pattern.

Is the actual dummy appropriate?

Compressive ankle forces can remain low when inducing midfoot fractures with a plantar impact that is directed parallel to the tibia axis. In these cases, much higher forces in the Chopart's joint were observed. The actual crash test models would not be able to detect the forces that caused midfoot fractures in these specific cases [11,17]. Even with the newest prototype (Thor LX), forces that were *only* directed in the longitudinal axis of the foot could not be detected. Of course, the new model can register *all* other forces, but based on our results, a significant influence of forces that were directed in the longitudinal axis of the foot on the incidence of midfoot fractures caused by plantar impact must be assumed. We are aware of the weaknesses of our study (pendulum vs. real-world crash, rigor mortis vs. muscle pretension, joint pressure/forces vs. "real forces", missing measurement of impact forces, acceleration and resulting forces, i.e., tibial load). The use of a pendulum may not be as realistic as a real-world crash, but the main problem in our study was that the pendulum did not allow the measurement of the effecting forces. We were only able to calculate the amount of energy that the pendulum had prior to the impact. If the rigor mortis really mirrors muscle pretension it has not been clearly determined by any study. Our main argument for the possible comparability of muscle pretension and rigor mortis and for the effectiveness of the pendulum is that we observed the same fracture pattern in our experimental study, accident analysis and clinical study [19,22]. Another main concern was if the measured joint forces did represent the real forces. There is no standard method available for a validation. Still, we believe that the introduced method allows an objective and reliable comparison of pressures and forces between ankle and Chopart's joint. The curved shape of Chopart's joint, which could principally redirect plantar forces into a longitudinal direction, may also cause these differences. Although we did not further analyze this effect, it may not be responsible for all pressures and forces that occurred in Chopart's joint. Consequently a considerable amount of force in the longitudinal axis of the foot can be assumed, and an influence of these forces on the incidence of midfoot fractures is probable. This calls into question the existing model for measurement of foot injury in crash testing. We recommend a modification of the foot dummy with an additional load cell that detects forces in the longitudinal direction of the foot axis. This dummy may be developed and calibrated with the introduced setting.

Acknowledgements

This work was supported in part by a grant from the "University Internal Achievement Support" from the Hannover Medical School, Hannover, Germany. The study was approved by the Ethical Commission of the Hannover Medical School, Hannover, Germany.

The manuscript was awarded by the German Orthopaedic Foot and Ankle Society with the 'Imhauser Award 2001' on April 6, 2001.

The authors thank Mrs. Birgitt Wiese (Institute for Biometry, Hannover Medical School, Hannover, Germany) for her help and support in carrying out the extensive statistical analysis and for her unbiased prior evaluation, and Eric Clarke, MD (Northtowns Orthopaedics, East Amherst, NY, USA) for revision and critical comments on the paper.

References

[1] Amon K. Luxationsfraktur der kuneonavikularen Gelenklinie. Klinik, Pathomechanismus und Therapiekonzept einer sehr seltenen Fussverletzung. Unfallchirurg 1990;93:431–4.
[2] Babst R, Simmen BR, Regazzoni P. Klinische Bedeutung und Behandlungskonzept der Lisfranc Luxation und Luxationsfraktur. Helv Chir Acta 1989;56:603–7.
[3] Brutscher R. Frakturen und Luxationen des Mittel- und Vorfusses. Orthopade 1991;20:67–75.
[4] Burgess AR, Dischinger PC, O'Quinn TD, Schmidhauser CB. Lower extremity injuries in drivers of airbag-equipped automobiles: clinical and crash reconstruction correlations. J Trauma 1995;38:509–16.
[5] Crandall JR, Martin PG, Sieveka EM, Pilkey WD, Dischinger PC, Burgess AR, et al. Lower limb response and injury in frontal crashes. Accid Anal Prev 1998;30:667–77.
[6] Davis BL, Cothren RM, Quesada P, Hanson SB, Perry JE. Frequency content of normal and diabetic plantar pressure profiles: implications for the selection of transducer sizes. J Biomech 1996;29:979–83.
[7] Dischinger PC, Kerns TJ, Kufera JA. Lower extremity fractures in motor vehicle collisions: the role of driver gender and height. Accid Anal Prev 1995;27:601–6.
[8] Fildes B, Lenard J, Lane J, Vulcan P, Seyer K. Lower limb injuries to passenger car occupants. Accid Anal Prev 1997;29:785–91.
[9] Graziano TA, Snider DW, Steinberg RI. Crush and avulsion injuries of the foot: their evaluation and management. J Foot Surg 1984;23:445–50.
[10] Hughes J, Pratt L, Linge K, Clark P, Klenerman L. Reliability of pressure measurements. Clin Biomech 1991;6:14–8.
[11] Jolly BT, Runge JW, Todd KH. NHTSA's new crash test dummy "Family". Ann Emerg Med 1999;33:719–22.
[12] Kallieris D, Mattern R, Wismans J. Stress and kinematic analysis of the head and neck in frontal collision. A comparison of voluntary probands and postmortem human test cadavers. Beitr Gerichtl Med 1989;47:235–41.
[13] Loo GT, Siegel JH, Dischinger PC, Rixen D, Burgess AR, Addis MD, et al. Airbag protection versus compartment intrusion effect

determines the pattern of injuries in multiple trauma motor vehicle crashes. J Trauma 1996;41:935–51.
[14] Mawhinney IN, McCoy GF. The crushed foot. J R Coll Surg Edinb 1995;40:138–9.
[15] McPhoil TG, Cornwall MW, Yamada W. A comparison of two in-shoe plantar pressure measurement systems. The Lower Extremity 1995;2:95–103.
[16] Myerson MS, McGarvey WC, Henderson MR, Hakim J. Morbidity after crush injuries to the foot. J Orthop Trauma 1994;8:343–9.
[17] Nyquist GW, Denton RA. Crash test dummy lower leg instrumentation for axial force and bending moment. ISA Trans 1979;18:13–22.
[18] Polliack A, Landsberger S, McNeal D, Sieh R, Craig D, Ayyappa E. Socket measurement system perform under pressure. Biomechanics 1999;6:71–80.
[19] Richter M, Thermann H, Otte D, Tscherne H. Foot fractures in restrained car front occupants. A long-term study over 23 years. J Orthop Trauma 2001;15(4):287–93.
[20] Richter M, Thermann H, Schratt E, Otte D, Tscherne H. Fractures of the foot and ankle in car drivers and passengers: incidence, analysis and long-term results. J Bone Joint Surg [Br] 1999;81-B(II):160.
[21] Richter M, Thermann H, vonRheinbaben H, Schratt E, Otte D, Zwipp H, et al. Frakturen der Fußregion bei PKW-Insassen. Häufigkeit, Ursachen und Langzeitergebnisse. Unfallchirurg 1999;102:429–33.
[22] Richter M, Wippermann B, Krettek C, Schratt E, Hufner T, Thermann H. Fractures and fracture dislocations of the midfoot occurence, causes and long-term results. Foot Ankle Int 2001; 22(5):392–8.
[23] Sangeorzan BJ, Ananthakrishnan D, Tencer AF. Contact characteristics of the subtalar joint after a simulated calcaneus fracture. J Orthop Trauma 1995;9:251–8.
[24] Suren EG, Zwipp H. Luxationsfrakturen im Chopart- und Lisfranc-Gelenk. Unfallchirurg 1989;92:130–9.
[25] Wagner UA, Sangeorzan BJ, Harrington RM, Tencer AF. Contact characteristics of the subtalar joint: load distribution between the anterior and posterior facets. J Orthop Res 1992;10:535–43.
[26] Wiley JJ. The mechanism of tarso-metatarsal joint injuries. J Bone Joint Surg [Br] 1971;53:474–82.
[27] Wilson DW. Injuries of the tarso-metatarsal joints. Etiology, classification and results of treatment. J Bone Joint Surg [Br] 1972;54:677–86.
[28] Wuelker N, Wirth CJ, Plitz W, Roetman B. A dynamic shoulder model: reliability testing and muscle force study. J Biomech 1995;28:489–99.
[29] Zwipp H, Dahlen C, Randt T, Gavlik JM. Komplextrauma des Fusses. Orthopade 1997;26:1046–56.